Anal. Chem. **2001,** *73,* 5485−5493

High-Sensitivity Instrument for Measuring Atmospheric NO_2

Yutaka Matsumi,* Shin-ichi Murakami, Mitsuhiko Kono,† and Kenshi Takahashi

Solar-Terrestrial Environment Laboratory and Graduate School of Science, Nagoya University, 3-13, Honohara, Toyokawa 442-8507, Japan

Makoto Koike

Department of Earth and Planetary Sciences, Graduate School of Science, The University of Tokyo, Hongo 113-0033, Japan

Yutaka Kondo

Research Center for Advanced Science and Technology, The University of Tokyo, Komaba 153-8904, Japan

We report on the development of a high-sensitivity detection system for measuring atmospheric NO_2 using a laser-induced fluorescence (LIF) technique around 440 nm. A tunable broad-band optical parametric oscillator laser pumped by the third harmonic of a Nd:YAG laser is used as a fluorescence excitation source. The laser wavelength is tuned at peak and bottom wavelengths around 440 nm alternatively, and the difference signal at the two wavelengths is used to extract the NO_2 concentration. This procedure can give a good selectivity for NO_2 and avoid interferences of fluorescent or particulate species other than NO_2 in the sample air. The NO_2 instrument developed has a sensitivity of 30 pptv in 10 s and S/N = 2. The practical performance of the detection system is tested in the suburban area for 24 h. The intercomparisons between the LIF instrument and a photofragmentation chemiluminescence (PF-CL) instrument have been performed under laboratory conditions. The correlation between the two instruments is measured up to 1000 pptv. A good linear relationship between the LIF measurements and the PF-CL measurements is obtained.

Nitric oxide and nitrogen dioxide (NO_x) play a critical role in determining levels of tropospheric O_3. The NO_x concentration also affects the abundance of hydroxyl OH radicals which are the main oxidizer in the troposphere. Then, the NO_x is a precursor of nitric acid, which can be a source of acid precipitation.[1] The measurement of reactive nitrogen species is a valuable tool in assessing photochemical processing that occurs in an air mass. There is still an urgent need to obtain understanding of the processes that govern the formation, removal, and distribution of tropospheric ozone and its precursors, including NO_x and other active nitrogen compounds. Therefore, measurements of NO_x in various sites and in various conditions are essential to understand the tropospheric chemistry. Mixing ratios of NO_x in the troposphere vary by more than 5 orders of magnitude from 100 ppbv (part per billion, 10^{-9}, by volume) levels in urban environments to a few pptv (part per trillion, 10^{-12}, by volume) levels in remote areas.[2] Especially in remote areas, it is important to measure the NO_2 concentrations with pptv resolution to understand the tropospheric ozone chemistry. For example, the transition from ozone formation to ozone destruction takes place at an NO_x level of the order of 10 pptv.[1,2]

For measurements of atmospheric NO_2, a variety of techniques have been developed. The photofragmentation chemiluminescence (PF-CL) technique provides sensitive, in situ, and single-point measurements.[3−6] In the PF-CL technique, NO_2 is converted to NO through the photolysis with irradiation of UV light (<400 nm). The resultant NO molecules are measured by the chemiluminescence from the electronically excited NO_2 which is produced by the reaction between NO and O_3. The PF-CL system measures both original NO in the sample air and NO converted from NO_2 with the irradiation of the photolysis UV light, while it detects only the original NO without the irradiation. The conversion efficiency from NO_2 to NO and NO detection sensitivity is calibrated with titration of the NO standard gas with O_3 gas. The

* Corresponding author: (fax) -81-533-89-5593; (e-mail) matsumi@stelab.nagoya-u.ac.jp.

† Present address: Atomic and Molecular Physics Laboratories, Research School of Physical Science and Engineering, The Australian National University, Canberra, ACT 0200, Australia.

(1) Finlayson-Pitts, B. J.; Pitts, J. N., Jr. *Chemistry of the Upper and Lower Atmosphere: Theory, Experiments, and Applications*; Academic Press: San Diego, 1999.

(2) Carroll, M. A.; Thompson, A. M. NO_x in the nonurban troposphere. In *Progress and problems in atmospheric chemistry*; Barker, J. R., Ed.; World Scientiffic: Singapore, 1995; pp 198−255.

(3) Fahey, D. W.; Hubler, G.; Parrish, D. D.; Williams, E. J.; Norton, R. B.; Ridley, B. A.; Singh, H. B.; Liu, S. C.; Fehsenfeld, F. C. *J. Geophys. Res.* **1986**, *91*, 9781−9793.

(4) Gao, R. S.; Keim, E. R.; Woodbridge, E. L.; Ciciora, S. J.; Proffitt, M. H.; Thompson, T. L.; McLaughlin, R. J.; Fahey, D. W. *J. Geophys. Res.* **1994**, *99*, 20673−20681.

(5) Harder, J. W.; Williams, E. J.; Baumann, K.; Fehsenfeld, F. C. *J. Geophys. Res.* **1997**, *102*, 6227−6243.

(6) Ryerson, T. B.; Williams, E. J.; Fehsenfeld, F. C. *J. Geophys. Res.* **2000**, *105*, 26447−26461.

10.1021/ac010552f CCC: $20.00
Published on Web 10/12/2001

conversion efficiency from NO_2 to NO has been reported to be 30−70%.[6] However, other nitrogen-containing species such as HONO, HNO_3, and peroxyacetyl nitrate (PAN) in the sample air may produce interfering signals through the photolysis. Various unsaturated hydrocarbons can also produce chemiluminescnce by reacting with O_3. The detection limit of the PF-CL technique for NO_2 was reported to be ∼20 pptv for a 10-s integration time when the signal-to-noise ratio (S/N) was 2.[5]

Bradshow et al.[7] reported a measurement system for NO_2 using a photofragment two-photon laser-induced fluorescence (PF-TP-LIF) instrument. In their system, NO_2 molecules in the sample air were photolyzed using the third harmonic of a Nd:YAG laser (355 nm). The resultant NO fragments were excited through the two-photon sequential photoabsorption process with 226-nm and 1.1-μm laser light. The fluorescence from the two-photon excited state of NO was detected at 190 nm.[8,9] They reported a detection limit of 8 pptv in 10 s. Here, adjusted values of the sensitivities in the literature are reported as those achieved in a 10-s integration time at an S/N of 2, assuming that the sensitivity is proportional to the square root of the integration time.

Tunable diode laser absorption spectroscopy (TDLAS) of NO_2 can provide in situ measurements.[10,11] To resolve a single absorption line and avoid interference from other species, the line width of the infrared diode laser in TDLAS for NO_2 was required to be $<2 \times 10^{-3}$ cm^{-1}. The detection limit of the TDLAS for NO_2 with a Herriot cell (equivalent path length 80 m) was reported to be 110 pptv for a 10-s integration time and S/N = 2.[11] The long-path absorption technique for NO_2 uses a system arrangement of total optical path length of more than several kilometers to obtain enough absorption intensity.[5] Recently, Garnica et al.[12] developed a detection system for atmospheric NO and NO_2 using an atmospheric pressure laser ionization (APLI) technique, which was based on time-of-flight mass spectrometry with resonance-enhanced multiphoton ionization (REMPI). Under laboratory conditions, the detection limit of the APLI system for NO_2 was 7 pptv for a 10-s integration time.[12]

George and O'Brien[13] developed a laser-induced fluorescence (LIF) technique for the detection of NO_2 with fluorescence assay by gas expansion (FAGE). The FAGE can reduce collisional quenching and lengthens fluorescence lifetimes due to low-pressure conditions, which also has been used in the detection of atmospheric OH radicals.[14−16] This allows temporal discrimination against the largely instantaneous background scattering signal occurring at the time of the laser pulse due to chamber and Rayleigh scattering processes. By operating at low pressures, the detection system can be turned on some time after the pulsed laser fires, since the fluorescence lifetime is much longer than the laser pulse width (∼5 ns). George and O'Brien[13] employed the second harmonic of the Nd:YAG laser at 532 nm as the excitation source for the NO_2 LIF detection. They used only one wavelength fixed at 532 nm. They obtained the detection limit of 1660 pptv under laboratory conditions with a signal collection time of 10 s and S/N = 2.[13] Matsumoto et al. developed a NO_2 instrument with a LIF technique using a Nd:YLF laser at 523.5 nm and reported the detection limit of 220 pptv for a 10-s integration time.[17]

Fong and Brune[18] also developed a FAGE system for the detection of NO_2 using a high-resolution tunable dye laser (10 kHz, 250 mW) pumped by a copper vapor laser. They excited the NO_2 sample at the two wavelengths alternatively around 564 nm. The two wavelengths correspond to peak and bottom positions of the absorption cross-section spectrum of NO_2. The measurements at the peak and bottom wavelengths can avoid the interference of fluorescent chemical species other than NO_2 in the sample air. However, since the absorption spectrum of NO_2 around 564 nm is very congested, the high spectral resolution for the laser system is required to separate the peak and bottom excitation points, which are separated by only 0.003 nm. The detection limit of the LIF system for NO_2 developed by Fong and Brune[18] was 1080 pptv in 10 s and S/N = 2.

Perkins and co-workers at Harvard University also developed an LIF NO_2 instrument for stratospheric measurements with ER-2 flights. The structure in the absorption band around 585 nm is used to measure the fluorescence intensities at the peak and bottom wavelengths. The estimated accuracy of their instrument was reported to be ±50 pptv at ±10% with a 10-s integration time. The simultaneous NO_2 observations with the Harvard University LIF instrument and a NOAA Aeronomy Laboratory PF-CL instrument showed a good correlation in POLALIS campaign flights.[19] Recently, Thornton et al.[20] reported a portable and autonomous LIF NO_2 instrument capable of measuring NO_2 throughout the troposphere, based on ideas used in the Harvard University LIF instrument. They used a dye laser (8 kHz, 100 mW) pumped by a diode-pumped YAG laser with a spectral resolution of 0.06 cm^{-1}. The sensitivity of their instrument was 15 pptv with a 10-s integration time and S/N = 2. The performance of the instrument developed by Thornton et al. was illustrated with observations at the field stations for 4−15 weeks.[20]

We have developed a single-point, in situ NO_2 instrument based on the FAGE technique with a broad-band optical parametric oscillator (OPO) laser. The laser system is wavelength tunable with a simple mechanism and is easy to operate. We used the features in the NO_2 absorption spectrum around 440 nm. The laser wavelength is tuned alternatively to the peak and the bottom

(7) Bradshaw, J.; Davis, D.; Crawford, J.; Chen, G.; Shetter, R.; Müller, M.; Gregory, G.; Sachse, G.; Blake, D.; Heikes, B.; Singh, H.; Mastromarino, J.; Sandholm, S. *Geophys. Res. Lett.* **1999**, *26*, 471−474.

(8) Bradshow, J. D.; Rogers, M. O.; Sandholm, S. T.; KeSheng, S.; Davis, D. D. *J. Geophys. Res.* **1985**, *90*, 12861−12873.

(9) Sandholm, S. T.; Smyth, S.; Bai, R.; Bradshaw, J. D. *J. Geophys. Res.* **1997**, *102*, 28651−28661.

(10) Schiff, H. I.; Karecki, D. R.; Harris, G. W.; Hastie, D. R.; Mackay, G. I. J. *Geophys. Res.* **1990**, *95*, 10147−10153.

(11) Webster, C. R.; May, R. D.; Trimble, C. A.; Chave, R. G.; Kendall, J. *Appl. Opt.* **1994**, *33*, 454−472.

(12) Garnica, R. M.; Appel, M. F.; Eagan, L.; McKeachie, J. R.; Benter, Th. *Anal. Chem.* **2000**, *72*, 5639−5646.

(13) George, L. A.; O'Brien, R. J. *J. Atmos. Chem.* **1991**, *12*, 195−209.

(14) Hard, T. M.; George, L. A.; O'Brien, R. J. *J. Atmos. Sci.* **1995**, 3354−3372.

(15) Mather, J. H.; Stevens, P. S.; Brune, W. H. *J. Geophys. Res.* **1997**, *102*, 6427−6436.

(16) Creasey, D. J.; Halford-Maw, P. A.; Heard, D. E.; Pilling, M. J.; Whitaker, B. J. *J. Chem. Soc., Faraday Trans.* **1997**, *93*, 2907−2913.

(17) Matsumoto, J.; Hirokawa, J.; Akimoto, H.; Kajii, Y. *Atmos. Environ.* **2001**, *35*, 2803−2814.

(18) Fong, C.; Brune, W. H. *Rev. Sci. Instrum.* **1997**, *68*, 4253−4262.

(19) Del Negro, L. A.; Fahey, D. W.; Gao, R. S.; Donnelly, S. G.; Keim, E. R.; Neuman, J. A.; Cohen, R. C.; Perkins, K. K.; Koch, L. C.; Salawitch, R. J.; Lloyd, S. A.; Proffitt, M. H.; Margitan, J. J.; Stimpfle, R. M.; Bonne, G. P.; Voss, P. B.; Wennberg, P. O.; McElroy, C. T.; Swartz, W. H.; Kusterer, T. L.; Anderson, D. E.; Lait, L. R.; Bui, T. P. *J. Geophys. Res.* **1999**, *104*, 26687−26703.

(20) Thornton, J. A.; Wooldridge, P. J.; Cohen, R. C. *Anal. Chem.* **2000**, *72*, 528−539.

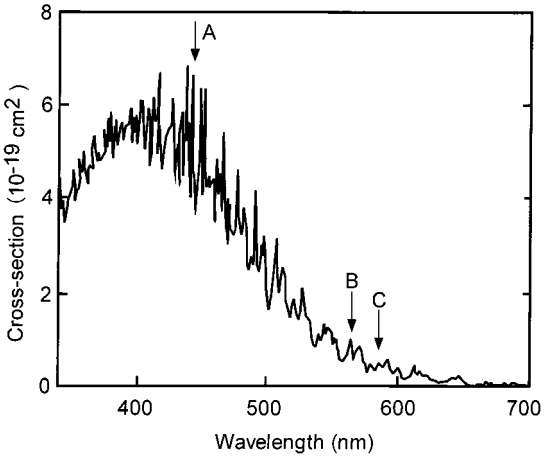

Figure 1. Low-resolution absorption cross-section spectrum of NO_2. The spectrum was taken from ref 21. The wavelength indicated arrow A (440 nm) is used in this work for the fluorescence excitation, while those indicated by arrows B (564 nm) and C (585 nm) are used in the fluorescence excitation by Fong and Brune[18] and by Cohen et al.,[20] respectively.

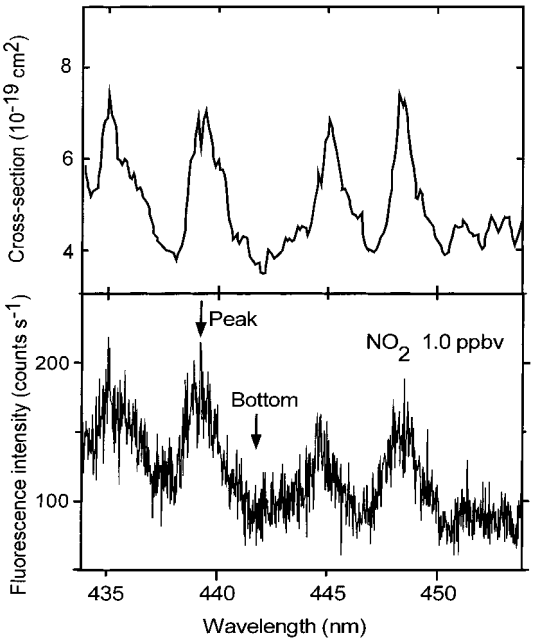

Figure 2. (a) Absorption cross-section spectrum of NO_2 around 440 nm. The spectrum was taken from the work by Schneider et al.[21] (b) Fluorescence excitation spectrum of NO_2 obtained in this work, when the fluorescence intensity was monitored scanning the wavelength of the broad-band OPO laser system. The peak and bottom wavelengths used to measure the NO_2 concentrations in this work are indicated with arrows.

wavelengths around 440 nm in the NO_2 absorption cross-section spectrum. The difference signal at the two wavelengths is measured to extract the NO_2 concentration. This procedure can give a good selectivity for NO_2 and avoid interferences by fluorescent or particulate species other than NO_2 in the ambient air. The NO_2 instrument developed has the sensitivity of 30 pptv in 10 s and S/N = 2. This sensitivity is as high as that of well-designed PF-CL instruments. The intercomparisons between our LIF instrument and a PF-CL instrument have been performed using standard gas and ambient air under laboratory conditions. A correlation between the two instruments is measured up to 1000 pptv. A good linear correlation between LIF and PF-CL measurements is obtained.

In field measurements, simultaneous measurements with instruments that are based on completely different detection principles are preferable to obtain reliable results. Our LIF instrument can be used with a PF-CL instrument in field campaigns, since its sensitivity and selectivity are as high as well-designed PF-CL instruments.

DESCRIPTION OF THE INSTRUMENT

Excitation System. We used the wavelength around 440 nm for the excitation of NO_2 molecule to detect the fluorescence. Figure 1 shows a low-resolution absorption spectrum of NO_2 in the whole visible wavelength region.[21] The excitation wavelength for LIF must be longer than 398 nm, which is the threshold wavelength for the dissociation

$$NO_2 + h\nu\ (\lambda < 398\ \text{nm}) \rightarrow NO + O$$

With the photoexcitation at wavelengths shorter than 398 nm, NO_2 gives no fluorescence.[22] Fong and Brune[18] used the rotational structure around 564 nm for the laser excitation wavelength in their LIF detection of NO_2. Thornton et al.[20] used the rotational structure around 585 nm. The absorption coefficient at 440 nm is ~10 times larger than that at 564 and 585 nm as shown in Figure 1. Figure 2a shows the detailed absorption spectrum of NO_2 in the wavelength region of 434−453 nm.[21] Figure 2b shows a fluorescence excitation spectrum of NO_2 measured with our laser system which will be described later. Since the difference in the LIF signals between the peak and bottom wavelengths is measured to extract the NO_2 concentration, the detection efficiency is higher when the ratio of the LIF signal intensities at the peak and bottom cross sections is larger. Around 440 nm, there is structure that is suitable for the peak and bottom measurements. As can be seen in Figure 2a, the ratios of the peak and bottom cross sections are about 1.6−2.0 in this spectral range, while that was 2.6 near 564 nm and ~3 near 585 nm.[18,20] The total detection limit of the instrument is proportional to the product of the absolute value of the absorption cross section and the ratio between the peak and bottom wavelengths. Therefore, use of the 440-nm region is still of great advantage, although the peak/bottom ratio is low. Furthermore, the peak and bottom features around 400 nm are separated by ~100 cm^{-1}. This means that a low-resolution tunable laser system can be used for excitation at peak and bottom wavelengths. On the other hand, the spectral bands at 564 and 585 nm have fine structures with less than 0.1-cm^{-1} intervals,[18,20] and high-resolution laser systems are required for selective tuning to the specific peak or bottom wavelength.

Figure 3 shows a schematic diagram of the NO_2 detection system that we have developed. The laser system consists of a broad-band OPO (optical parametric oscillator, Continuum, Surelite-OPO) that is pumped by the third harmonic (355 nm) of a Nd:YAG laser (Continuum, Surelite II). The 355-nm light from

(21) Schneider, W.; Moortgat, G. K.; Tyndall, G. S.; Burrows, J. P. *J. Photochem. Photobiol.* **1987**, *40*, 195−217.

(22) Okabe, H. *Photochmeistry of small molecules*; John Wiley & Sons: New York, 1978; p 130.

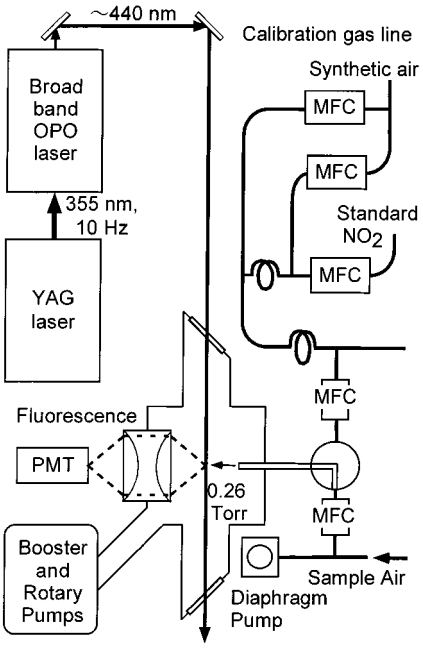

Figure 3. Schematic diagram of the NO_2 instrument developed in this work.

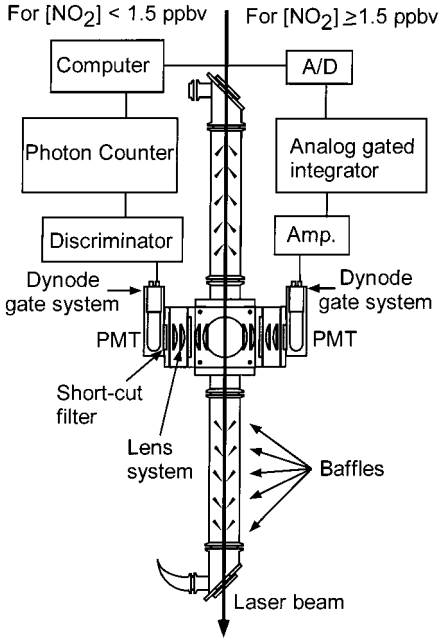

Figure 4. Cross section of the fluorescence cell and fluorescence detection systems. When the concentration of NO_2 is lower than 1.5 ppbv, the output of a PMT is fed into a discriminator and photon counter system (left-hand side). When the concentration of NO_2 is high than 1.5 ppbv, the output of another photomultiplier, which is located in the opposite side of the other one, is fed into an amplifier and analog gated integrator system (right-hand side). The data from both systems are processed with a microcomputer, which also controls the wavelength of the OPO laser system.

the YAG laser provides ~170 mJ pulse^{-1} at the repetition rate of 10 Hz. The energy of the OPO laser light around 440 nm is ~10 mJ pulse^{-1} at 10 Hz (100 mW) at the excitation point in the fluorescence cell. The time width of the OPO laser pulse is ~5 ns. The OPO laser light is always monitored at the exit position of the fluorescence cell with a power meter (Scientech, AC2501). The broad-band OPO contains only one BBO crystal, and the wavelength of the broad-band OPO system is tuned by the angle of the crystal. The angle of the BBO crystal for the OPO is driven by a linear actuator (Sigma Koki, DMY-25) with a sine bar. The position of the linear actuator is computer controlled. The transit time for changing the OPO wavelength between the peak and bottom wavelengths is less than 0.2 s. Since the OPO laser is solid state and does not need a circulation system of liquid dye solution, it is easy to operate.

The line width of the OPO laser light at 440 nm was measured to be 21 cm^{-1}, using a monochromator ($f = 500$ mm). Figure 2b shows the fluorescence excitation spectrum of NO_2 with the OPO−YAG laser system under the condition of the NO_2 concentration of 1.0 ppbv, where the OPO laser wavelength is scanned while the fluorescence intensity is monitored with a photomultiplier. The structure of the absorption spectrum shown in Figure 2a is well reproduced in the excitation spectrum with the broad-band OPO laser system. This indicates that the spectral resolution of the broad-band OPO system (21 cm^{-1} equivalent to ~0.41 nm) is sufficient to separate the spectral peak and bottom positions in the NO_2 spectrum around 440 nm. We have chosen 439.5 nm for the peak wavelength and 442.0 nm for the bottom wavelength. The ratio of the fluorescence intensities at the peak and bottom wavelengths is ~1.8, which is in good agreement with the cross-section ratio at the two wavelengths in Figure 2a. This indicates that the photoabsorption of NO_2 is not saturated by the excitation laser light with power of 10 mJ pulse^{-1} in this wavelength region. For the peak absorption cross section of 7×10^{-19} cm^2 at 439.5 nm and laser power of 10 mJ pulse^{-1} with the beam diameter of 10 mm, it is estimated that ~2% of NO_2 molecules in the laser irradiation zone is photoexcited.

Fluorescence Monitoring System. Figure 4 shows a detailed schematic diagram of the fluorescence cell and the signal detection systems. Optical baffles with cone-shaped apertures are placed within both arms of the fluorescence cell to minimize detection of light scattered by the entrance and exit windows. The diameters of the aperture holes are 12 mm in the entrance baffle arm and 14 mm in the exit baffle arm. The diameter of the laser beam is expanded to 10 mm by a lens system before entering into the fluorescence cell to reduce the laser power density and to avoid saturation of the photoabsorption of NO_2. We have used a single-pass cell, while Thornton et al.[20] used a multipass White cell with a narrow laser beam. The excitation efficiency of the single-pass cell is lower than that of the multipass cell. Since our laser system is operated at low repetition rate (10 Hz) with average power of 100 mW, we have to use the large-diameter beam (10 mm) to avoid saturation. It is impossible to use the multipass cell with the large-diameter laser beam. The laser system used by Thornton et al.[20] was operated at a high repetition rate (8 kHz) with the average power of 100 mW and each laser pulse has low power, which did not saturate the optical absorption of NO_2 even with the narrow laser beam.

For the detection of the fluorescence from NO_2, two red-sensitive photomultiplier tubes (PMTs, Hamamatsu R3896) are used. This type of PMT has a multi-alkali photocathode, which is sensitive in the wavelength range up to 820 nm with a quantum efficiency of more than 5%. The emitting image of the NO_2 volume along the excitation laser beam in the cell is focused onto the

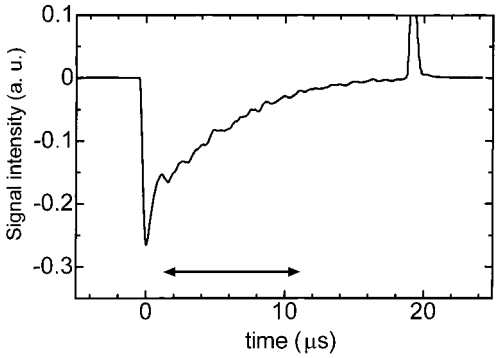

Figure 5. Time profile of the fluorescence signal from the phomultiplier with the dynode gate system and the amplifier. The trace was measured with a digital oscilloscope with an accumulation of 256 traces. The mixing ratio of NO_2 sample is 100 ppbv, and the cell pressure is 0.26 Torr. The arrow indicates the gate time of the analog integrator. The positive spike noise at $t = 20$ ms appears, and the negative spike noise at $t = 0$ appears. These electronic noise peaks are produced by the dynode gate system.

photocathode of each PMT by a set of four quartz lenses (50 mm diameter, $f = 100$ mm). To avoid detection of the chamber and Rayleigh scattering, a long-pass optical filter of $\lambda > 500$ nm (CVI, LPF-500) is equipped in front of each PMT. Since the fluorescence lifetime of NO_2 ($\sim$5 μs) is much longer than the laser pulse time width ($\sim$5 ns), dynode gate systems in the PMT sockets (Hamamatsu, C1392−56) are also used to eliminate the chamber and Rayleigh scattering light. The sensitivity of the PMTs is normally kept off and is turned on from 200 ns after the laser pulse with a duration time of 20 μs. The rise time of the PMT sensitivity is 20 ns (10−90%) at the opening of the dynode gate.

The outputs of the PMTs are processed by two methods: one is a photon-counting method and the other is an analog gated-integration method, which are presented in the left- and right-hand sides of Figure 4, respectively. When the mixing ratio of NO_2 in sample air is low (<1.5 ppbv), a photon-counting method is used. The output of the one PMT is fed into a discriminator (Hamamatsu C3866) with a time resolution of 25 ns and then photoelectron pulses are counted by a fast counter board (Hamamatsu M3949, maximum count rate, 5×10^7 count s^{-1}) which is slotted into the microcomputer. To avoid counting of the switching noise of the dynode gate system, the gate of the photon counter is opened at 250 ns after the laser pulse. The counting gate width is 10 μs. When the mixing ratio of NO_2 in sample air is high (>5 ppbv), pileup phenomena were observed since intervals of the photoelectron pulses exceed the time resolution of the photon counting system. For measurements of high-NO_2 mixing ratios ($\geq$1.5 ppbv), the output of the other PMT is amplified and fed into an analog gated integrator (Stanford Research, SR250) with the integration over 10 successive laser pulses. The gate of the integrator is opened at 1 μs after the laser pulse and its duration is 10 μs. The integrated signal is sampled with an A/D board and the microcomputer. Since the photon counting system is more suitable for signal accumulations for long time than the analog integration system, the counting system is used when the NO_2 mixing ratio is lower than 1.5 ppbv.

The emission wavelength of the NO_2 fluorescence extends over 1000 nm, even when the excitation wavelength is 440 nm. A GaAs photocathode PMT (Hamamatsu, R636-10) was also tested, which had larger quantum effciency at wavelengths of >900 nm than the multi-alkali PMT (Hamamatsu, R3896). We compared the wavelength sensitivities of the PMTs by monitoring the actual NO_2 fluorescence with various short cutoff filters (600, 700, and 800 nm). The quantum efficiency of the GaAs PMT was $\sim$50% more for the NO_2 emission at long wavelengths than that of the multi-alkali PMT. However, the GaAs PMT had some disadvantages. The geometrical size of the GaAs PMT photocathode was much smaller (3 × 12 mm) than that of the multi-alkali PMT (8 × 24 mm). This resulted in the lower collection efficiency, since the image size of 10-mm diameter for the NO_2 fluorescence could not focused into a small point with the lens system. The gain of the GaAs PMT was much lower, and its thermal noise was larger than the multi-alkali PMT. The overall sensitivity of the detection system with the GaAs PMT was lower than that with those of the multi-alkali PMT. Therefore, we have chosen to use the multi-alkali PMT (R3896). The PMT was not cooled, since the dark count rate of the multi-alkali PMT was less than 0.1 counts s^{-1} with the gate time width of 10 μs at the repetition rate of 10 Hz even at room temperature.

Gas Handling System. Ambient air is pulled into the fluorescence cell with a booster pump (ULVAC PMB001C) and a rotary pump (Alcatel 2021). The pumping speed at a cell pressure of 0.26 Torr is $\sim$2000 L min^{-1}. The pressure in the cell is monitored with a capacitance manometer (MKS Baratron 122A, full scale 2 Torr). The sample flow rate in the fluorescence cell is 1.3 standard liter per minute (slm). The flow rate in the fluorescence cell is high enough to avoid irradiation of an air sample by two successive laser pulses before it leaves the detection volume. For calibration of the detection system, NO_2 from a standard mixing ratio gas cylinder (Nihon Sanso, 9.82 ppmv) is diluted with the synthetic air flow. Flow rates of all the gases are controlled by mass flowmeters. All the mass flowmeters are calibrated using a soap film flowmeter (STEC, SF1). The weight and size of the whole system of our prototype instrument are about 250 kg and 2 m width × 1 m depth × 1 m height, respectively.

INSTRUMENT PERFORMANCE

Instrument Sensitivity. The fluorescence lifetime, τ_f, of NO_2 depends on the pressure in the cell:

$$\tau_f = 1/k_f = 1/(k_r + \sum k_q^M [M]), \quad (1)$$

where k_r is a radiative rate constant of the photoexcited NO_2 and k_q^M is a quenching rate constant for M such as O_2 and N_2. The radiative lifetime of NO_2 is $\sim$70 μs with the excitation around 440 nm,[23] which corresponds to $k_r \sim 1.5 \times 10^4$ s^{-1}. Figure 5 shows a typical time profile of the fluorescence signal of NO_2 from the PMT with the dynode gate system and analog amplifier, which was measured with a digital oscilloscope (Tektronics, TDS380P, 400 MHz) with an accumulation of 256 traces when the NO_2 concentration was 100 ppbv and the pressure in the cell was 0.26 Torr. The time profile indicates the fluorescence lifetime is estimated to be $\sim$5 μs at a pressure of 0.26 Torr.

The detection sensitivity of FAGE-LIF instruments, S_{NO_2}, is proportional to the product of the fluorescence quantum yield,

(23) Donnelly, V. M.; Kaufman, F. *J. Chem. Phys.* **1978**, *69*, 1456−1460.

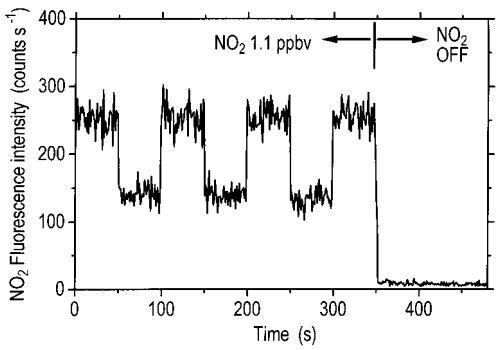

Figure 6. Typical example of the photon counting measurements of the fluorescence intensities with our NO_2 instrument. The sample NO_2 gas concentration is 1.1 ppbv, which is generated by the dilution of the standard NO_2 gas with the synthetic air. The fluorescence is measured while alternatively tuning the laser wavelength at the peak (439.5 nm) and bottom (442.0 nm) positions every 50 s. Then, the NO_2 gas is reduced to zero to measure the background signal intensity. The fluorescence intensity is normalized for the excitation laser power of 100 mW.

Φ_f, and the ratio of the pressures in the fluorescence cell and in the ambient air, P_{cell} and $P_{ambient}$:

$$S_{NO_2} \propto \Phi_f(P_{cell}/P_{ambient}) \quad (2)$$

The fluorescence quantum yield of NO_2 in the cell is determined by the equation

$$\Phi_f = k_r/(k_r + \sum k_q^M [M]) \quad (3)$$

The quenching rate constant by N_2 and O_2 were reported to be $\sim 5 \times 10^{-11}$ cm^3 molecule^{-1} s^{-1}.[24] Under the pressure condition of >0.1 Torr, quenching by the air molecules is much larger than the radiative lifetime; that is, $k_r \ll \sum k_q^M$ [M]. Therefore, the signal loss by the pressure lowering and the gain of the fluorescence quantum yield cancel each other. The signal intensity is proportional to the NO_2 mixing ratio and not to its absolute number density in the ambient sample air. At the total pressure of 0.26 Torr used in this study, the value of Φ_f is estimated to be 0.07.

Figure 6 shows a typical example of the photon counting measurements of the fluorescence intensities with our NO_2 instrument, when the NO_2 gas concentration was 1.1 ppbv. The vertical scale is the fluorescence intensity in counts per unit time (counts s^{-1}), and the horizontal axis is time. The OPO laser wavelength was fixed at the peak position of the NO_2 absorption (439.5 nm) for 50 s and then the wavelength was changed and fixed at the bottom position (442.0 nm) for 50 s. The measurements at the peak and bottom positions were alternatively repeated several times. Then, the NO_2 gas concentration was reduced to zero to measure the background signal intensity. The fluorescence intensities at the peak and bottom wavelengths versus NO_2 concentrations with the standard gas sample in the range of 0−1.25 ppbv are plotted in Figure 7, which were measured by the photon counting system. The slopes of the plots for the peak

(24) Donnelly, V. M.; Keil, D. G.; Kaufman, F. *J. Chem. Phys.* **1979**, *71*, 659−673.

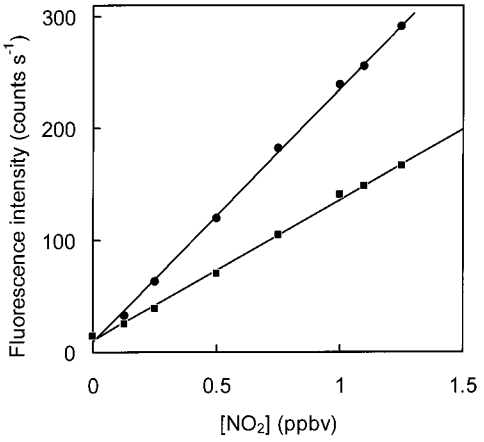

Figure 7. Calibration plots for the peak (circles) and bottom (squares) wavelengths with the photon counting system. The laser wavelengths are 439.5 and 442.0 nm for the peak and bottom positions, respectively. The concentration range of NO_2 is 0−1.25 ppbv. The slopes of the plots for the peak and bottom wavelengths are C_{peak} = 0.229 and C_{bottom} = 0.128 in counts s^{-1} pptv^{-1}, respectively. The fluorescence intensity is normalized for the excitation laser power of 100 mW.

and bottom wavelengths were $C_{peak} = 0.229$ and $C_{bottom} = 0.128$ in counts s^{-1} pptv^{-1}, respectively, and the ratio of the slope, C_{peak}/C_{bottom}, was 1.79.

Figure 8 shows plots of the fluorescence intensities at the peak and bottom wavelengths versus NO_2 concentrations, which were measured with the analog gated integrator. The ratio of the slopes at the peak and bottom wavelengths was 1.82, which is in good agreement with the results with the counting system. This indicates that the measurement system has a linearity in the wide range of NO_2 concentrations up to 140 ppbv.

Minimum Detectable Limit. When the predominant source of noise is fluctuations of the photon counting values with Poisson distributions, the minimum detectable NO_2 mixing ratio of the instrument, $[NO_2]_{min}$, is expressed by

$$[NO_2]_{min} = \frac{S/N\sqrt{S_{bg}}}{\sqrt{t}(C_{peak} - C_{bottom})} \quad (4)$$

where S/N is the required signal-to-noise ratio, S_{bg} is the background signal level of the instrument (in counts s^{-1}), and t is the averaging time of the instrument (in s). The background signal level was 10.1 counts s^{-1}. When the laser light was cut before the fluorescence cell, the photon counting level was zero. Therefore, the background signal came mainly from the wall and Rayleigh scattering of the laser light. The background level was stable on the time scale of the on/off measurements. With S/N = 2, the minimum detectable limit of our NO_2 instrument is calculated to be 30 pptv with the integration time of t = 10 s and 5.5 pptv with t = 300 s. The minimum detectable limit obtained for our LIF instrument is estimated to be as low as those of well-designed PF-CL instruments. The minimum detectable limit of our instrument is a little higher than that reported by Thornton et al.[20] (15 pptv 10 s). This is mainly due to the lower background level of their instrument (1.2 counts s^{-1}). In the future, we will try to reduce the background level to lower the minimum detectable limit.

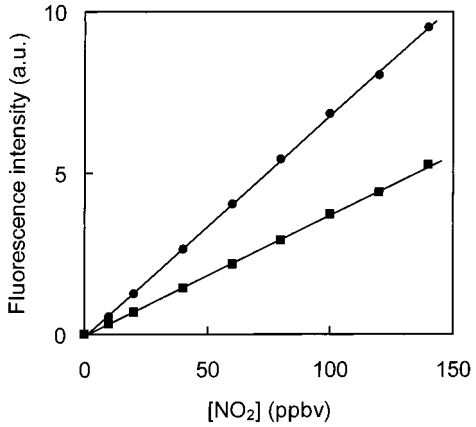

Figure 8. Calibration plots for the peak (circles) and bottom (squares) wavelengths with the analog gated integrator system. The laser wavelengths are 439.5 and 442.0 nm for the peak and bottom positions, respectively. The concentration range of NO_2 is 0−140 ppbv. The fluorescence intensity is normalized for the excitation laser power of 100 mW.

Possible Interferences. The possible fluorescent species with excitation around 440 nm are compounds such as large aromatics and molecules with many unsaturated bonds. Interference from species other than NO_2 can be eliminated by tuning the laser wavelength at the top and bottom wavelengths in the NO_2 absorption. There are some molecules that produce NO_2 by photodissociation such as HNO_3, NO_3, N_2O_5, HNO_4, PAN, $ClONO_2$, $ClNO_2$, and ClONO. The energy threshold of HNO_3 to photodissociate to NO_2 + OH is ∼600 nm. However, the absorption cross section of HNO_3 is extremely small in the visible region, which is 1×10^{-23} cm^2 even at 340 nm.[25] The absorption cross section of NO_2 at the laser wavelength used in our instrument (440 nm) is $\sim 7 \times 10^{-19}$ cm^2.[21] The photodissociation threshold wavelength of NO_3 to NO_2 + O is also ∼600 nm. The absorption cross section of NO_3 at 440 nm is $\sim 7 \times 10^{-19}$ cm,[2,22] which is almost as large as that of NO_2. However, the fluorescence efficiency from NO_3 with the two-step process of photodissociation to produce NO_2 and excitation of the produced NO_2 for LIF in a single laser pulse should be smaller than the fluorescence efficiency of the original NO_2 with the one-photon process. Even for the photodissociation process of NO_3, the photoabsorption with 7×10^{-19} cm^2 must not be saturated with the laser power density used in our instrument. The production of NO_2 from N_2O_5, HNO_4, $ClONO_2$, $ClNO_2$, and ClONO at 440-nm laser light cannot interfere with the LIF detection of NO_2 at 440 nm, since the absorption cross sections of these molecules are 10−100 times smaller than that of NO_2 at 440 nm and the concentrations of these compounds are not so much higher than that of NO_2.[1] The concentration of PAN can be 10−100 times higher than that of NO_2. However, the absorption cross section of PAN at 440 nm is estimated to be more than 10^4 times smaller than that of NO_2, according to the cross section at the longer wavelength edge of the UV absorption band of PAN (350 nm).[25] Therefore, the interference by PAN can be also ignored.

(25) DeMore, W. B.; Sander, S. P.; Golden, D. M.; Hampson, R. F.; Kurylo, M. J.; Howard, C. J.; Ravishankara, A. R.; Kolb, C. E.; Molina, M. J. *Chemical Kinetics and Photochemical Data for Use in Stratospheric Modeling*; JPL Publication 97-4, NASA, Calif. Inst. Technol.: Pasadena, CA, 1997; Vol. 12.

The fluorescence of NO_2 is quenched by water molecules as well as air molecules. The change of H_2O concentration in the ambient air is large under various conditions. The quenching rate constant of NO_2 excited state by the collisions with H_2O is ∼6 times larger than that with air.[24] At a pressure of 0.26 Torr in the cell, the fluorescence quantum yield of NO_2 is reduced ∼9% by the presence of 3% v/v H_2O, which corresponds to a relative humidity of 100% at 298 K. Since this negative interference by water vapor is quantitative, it can be corrected by the simultaneous measurements of NO_2 and H_2O in sample air, when very accurate values of NO_2 concentration are necessary.

AMBIENT MEASUREMENT

Ambient measurements were performed on May 15 and 16, 2000 for 24 h in the south yard on the Toyokawa campus of Nagoya University. The sampling point is located at 2.0 m height from the ground and 10 m south from the laboratory building which is ∼9 m tall. The yard is covered with lawn and has an area of ∼4000 m^2. Toyokawa campus is located in a suburban factory area and Tomei expressway runs 1 km north of the campus. Along with NO_2, O_3 and sunlight UV-A were monitored with commercial instruments. The concentration of O_3 was measured with Thermo-Electron model 49 and sunlight UV-A with Eiko Seiki MS-210A.

The length of the PTFE tube (inner diameter, 4 mm) from the sampling point to the fluorescence cell is ∼15 m. A PTFE filter with a pore size of 1.2 μm (Millipore, 80 mm diameter) is installed at the top of the sampling tube to remove particles that can cause large laser light scattering. The loss of NO_2 in the PTFE filter was checked using standard gas of 10 ppbv concentration, and the LIF signal intensity was unchanged with and without the filter. The ambient air is aspirated through the tube with a diaphragm pump (ULVAC DA-50) at the rate of 6 L min^{-1} (Figure 3). The residence time in the 15-m tube was ∼0.6 s from the outside sampling point to the fluorescence cell. This residence time in the tube was estimated to be much shorter than the reaction time between NO and O_3 (60 ppbv) in the sample air (>30 s). In the measurements, the laser wavelength was tuned at the top and bottom absorption positions, 439.5 and 442.0 nm, alternatively, every 50 s. The analog sampling mode was used for processing of the PMT signal, since the ambient NO_2 mixing ratio is in the range of 5−30 ppbv. The NO_2 instrument was calibrated by replacing the ambient air with the standard NO_2 gas of 10−30 ppbv about every 16 min throughout the measurements. Every calibration procedure took ∼200 s, and the measurements were interrupted during that time. The sensitivity factor of the instrument varied within 4.5% during the 24-h measurement time. The laser power was almost constant, and no additional optical adjustment of the laser system was required during the 24-h measurement.

Figure 9 shows the results of the ambient measurements for 24 h. The top panel presents the NO_2 mixing ratios measured with our LIF instrument, while the middle and bottom panels indicate the O_3 mixing ratios and UV-A intensities, respectively. The mixing ratio of O_3 during the nighttime is very low, compared with the daytime level. The depletion of O_3 during the nighttime should be due to surface deposition in a thin inversion layer near the ground in addition to the reaction NO + O_3 → NO_2 + O_2. After sunrise, O_3 is produced by photochemical processes and

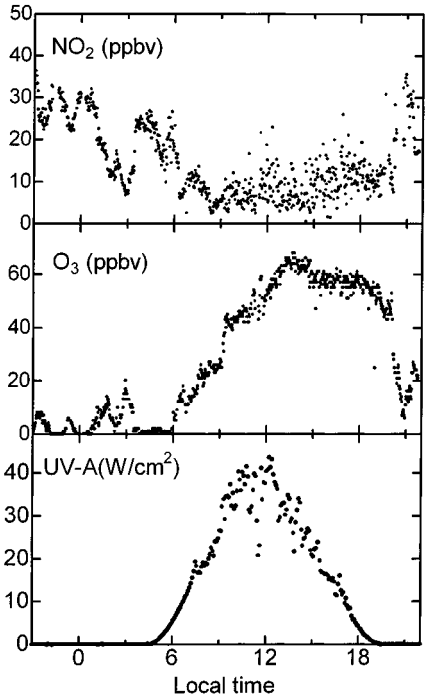

Figure 9. Results of ambient measurements for 24 h on May 15 and 16, 2000. The top panel presents the NO_2 mixing ratios measured with our LIF instrument, while the middle and bottom panels indicate the O_3 mixing ratios and UV-A intensities, respectively.

its mixing ratio rises rapidly. The spike features of the NO_2 mixing ratios during the daytime may be attributed to nearby traffic. The changes in NO_2 concentration may be due to changes in the boundary layer height.[26] The NO_2 level started to decrease from sunrise. The relatively low level of NO_2 during the daytime is due to photolysis by sunlight and convective mixing in the boundary layer. During the night, the NO_2 mixing ratio did not vary so much, but had an inverse correlation with O_3. This inverse correlation may be attributed to the wind direction changes bringing air masses of different origins.

INTERCOMPARISON WITH THE PF-CL INSTRUMENT

The intercomparison between the LIF instrument and a PF-CL instrument was made in the laboratory in Toyokawa. The PF-CL instrument was built by Kondo and co-workers and used in the BIBLE-B campaign in 1999 and SOLVE campaign in 1999−2000. The design of the PF-CL instrument was based on the photolysis system reported by Gao et al.[4] Briefly, the PF-CL system has three chemiluminescence detection (CLD) systems. The first CLD system was equipped for NO detection in the sample air, the second was for detection of NO_2 through the photolysis converter cell, and the third was for the detection of NO_y through a heated gold tube for catalytic conversion of NO_y to NO with CO gas. The photolysis light source to convert NO_2 to NO was a metal halogen lamp of 400-W input power with a filter system that transmitted light of wavelengths longer than 340 nm. The mixing ratio of NO was simultaneously measured with the CLD system for NO. The NO_2 mixing ratio was calculated by

$$[NO_2] = (I_{NO_2}/S_{NO_2} - [NO])/\alpha \quad (5)$$

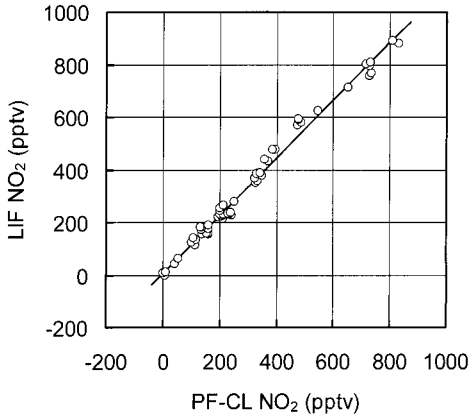

Figure 10. Mixing ratios measured with the LIF instrument versus those with the PF-CL (photofragmentation chemiluminescence) instrument. The straight line indicates the least-squares regression line.

where I_{NO_2} and S_{NO_2} are the signal intensity and sensitivity factor of the CLD system for NO_2, respectively, [NO] and [NO_2] are the mixing ratios of NO and NO_2 in the sample air, respectively, and α represents the conversion efficiency with the photolysis cell. Every 10 s, the [NO] and [NO_2] signals were accumulated and [NO_2] was calculated. The sensitivity factors of the NO and NO_2 CLD systems and the conversion efficiency were calibrated every 5 min at the mixing ratio of [NO] = 938 pptv and [NO_2] = 822 ppbv. The NO_2 standard gas is in-line synthesized NO_2 from NO gas with a standard NO gas cylinder (Nihon Sanso, 8.04 ppmv) and excess ozone gas. The ozone gas is produced by the photolysis of oxygen with an Hg 185-nm light.

In the LIF measurements, the laser wavelength was fixed at the top and bottom absorption positions, 439.5 and 442.0 nm, alternatively, every 20 s. The measurements was done with the photon counting mode, since the mixing ratio of NO_2 used in the intercomparison is less than 1.5 ppbv. The NO_2 mixing ratios were calculated from the differences between the signals between the top and bottom wavelengths. The sensitivity of the LIF instrument was calibrated every 60 min at the NO_2 mixing ratio of 862 pptv, which was generated from the standard NO_2 cylinder by dilution with the synthetic air. The mixing ratio of the sample NO_2 used in the intercomparison was in the range up to ~1000 pptv. The synthesized NO_2 produced from the reaction between the standard NO cylinder gas and ozone and then diluted with the synthesized air was used as the sample gas. The conversion ratio from NO to NO_2 was monitored by the CLD NO instrument, which was kept ~50%. The ambient air diluted with the synthesized air was also used as sample gas for the intercomparison experiments. The mixing ratios of NO_2 and NO in the ambient air were about 20 and 7.5 ppbv during the measurements.

The mixing ratio measured with the LIF instrument versus that with the PF-CL instrument are plotted in Figure 10. The data in Figure 10 include the results with both synthetic NO_2 and diluted ambient air. The least-squares regression line is also indicated in Figure 10. The linear regression analysis could be described by the equation

(26) Rohrer, F.; Brüning, D.; Grobler, E. S.; Weber, M.; Ehhalt, D. H.; Neubert, R.; Schüssler, W.; Levin, I. *J. Atmos. Chem.* **1998**, *31*, 119−137.

$$[\mathrm{LIF}] = (1.09 \pm 0.05)[\mathrm{PF\text{-}CL}] + (9.0 \pm 11.6), \quad \text{in pptv} \quad (6)$$

with a correlation factor of $R^2 = 0.989$, where [PF-CL] and [LIF] are the NO_2 mixing ratios measured with the PF-CL and LIF instruments, respectively. The errors indicate 1σ uncertainties. For the data below 400 ppt, the linear regression line was expressed as

$$[\mathrm{LIF}] = (1.07 \pm 0.06)[\mathrm{PF\text{-}CL}] + (6.4 \pm 13.2), \quad \text{in pptv} \quad (7)$$

with a correlation factor of $R^2 = 0.967$.

The correlation factors close to 1 indicates the excellent linearity between the LIF and PF-CL measurements. The values of the regression slopes include the uncertainty of the standard gas concentrations, since the two instruments were calibrated with the different standard gases. The intercepts are almost zero within the uncertainties.

SUMMARY

The new NO_2 instrument was developed using the FAGE-LIF technique. The wavelengths for the peak and bottom features of NO_2 around 440 nm were used for the fluorescence excitation of NO_2, while previous studies used features at 564 and 585 nm. The usage of 440 nm for the excitation has several advantages over the longer wavelength excitation at 564 and 585 nm: (1) The efficiency of the photoexcitation of NO_2 is higher, since the value of the peak photoabsorption cross section multiplied by the peak bottom cross-section ratio at the features around 440 nm is several times larger than those around 564 and 585 nm. (2) The detection efficiency of the NO_2 fluorescence using a low-noise photomultiplier with a multi-alkali photocathode is higher than the longer wavelength excitations, since the fluorescence emits in the shorter wavelength range where the quantum efficiency of the photomultiplier is high. (3) The peak and bottom features in the absorption spectrum of NO_2 are more separated (100 cm^{-1}) than those around 564 and 585 nm (<0.1 cm^{-1}). This makes it possible to use the broad-band OPO laser. (4) Since the broad-band laser can interact with many rotational states of NO_2, the saturation level of the laser excitation is high and a strong fluorescence signal can be obtained.

The NO_2 instrument developed in this study has the following features: (1) single-point, in situ measurement, (2) high sensitivity of the 30 pptv in 10 s and S/N = 2, which is high enough for measurements under remote air conditions, (3) high selectivity for NO_2 using the two-wavelength measurements and no possibility of interferences by other species even with photodissociation processes, (4) wide-range signal linearity from a few tens of pptv to sub-ppmv levels, (5) fast response of less than 1 s, and (6) simple and easy-to-operate laser system. These features suggest the NO_2 instruments developed is suitable for the ground and air-borne measurements in clean remote and urban area.

The intercomparison between the LIF instrument and a PF-CL instrument was made in the laboratory. A good linear correlation between the LIF and PF-CL instruments was obtained.

ACKNOWLEDGMENT

This work was supported by the Toyota High-Technology Research Grant Program. Support of this work by Grant-in-Aid for Scientific Research from the Ministry of Education, Culture, Sports, Science and Technology, Japan, is also acknowledged. We also thank Akiyuki Takegawa and Noriji Toriyama of the Solar-Terrestrial Environment laboratory, Nagoya University, for their technical supports and advice.

Received for review May 15, 2001. Accepted August 20, 2001.

AC010552F